Flow Analysis with Digital Subtraction Angiography:
2. Acquisition and Accuracy of Transit-Flow Measurements

John R. Hesselink[1, 2]
Kee Hyun Chang[1]
Kyung J. Chung[2, 3]
Lauren Abbate[1]
Mitchell Goodsitt[1]

A steady-state flow model was used to optimize methods of data analysis, to investigate variables that affect the time-density curves, and to determine the accuracy of transit-flow measurements with digital subtraction angiography. The most accurate data were obtained by using a small region of interest placed within the vessel, averaged data acquisition, and a gamma-variate fit applied to the time-density curve. The integrated area of the curve depended on the flow, vessel size, amount of iodine injected, framing rate, and the kVp. The integrated area was not affected by the mAs; the matrix size; or the volume, concentration, or rate of injection of the contrast material. Subject density, image intensifier mode, and field size did not affect the curves except for their contribution to scatter and beam hardening. There was good corrrelation between digital subtraction angiographic transit-flow measurements and known flow values.

Digital subtraction angiography (DSA) lends itself to flow analysis because the data are in a digital format. Regional density measurements of a series of consecutive images can be rapidly calculated and displayed as time-density (T-D) curves. A flow model for use with DSA was described in our companion article [1]. Initial tests prove that the model gives reproducible results and responds appropriately to changing flow rates.

There are a number of operator-controlled variables associated with DSA flow analysis that affect the T-D curves and, thus, flow calculations. The integrated area of the T-D curves is inversely proportional to flow and directly related to the amount of iodine injected and the cross-sectional area of the vessel [2]. We conducted experiments to determine the effect of other variables, including methods of T-D curve analysis, kVp, mAs, framing rate, subject density, matrix size, and image-intensifier mode. Finally, the flow model was used to determine the accuracy of DSA transit-flow measurements in a controlled laboratory setting.

Methods

For the assessment of different methods of accumulating flow data, 10 DSA runs were performed with the flow model by using a standard technique of 70 kVp, 200 mA, and 0.024 sec. The images were acquired at 4 frames per sec for 10 sec on a 256 × 256 matrix with a 4-in. (10-cm) mode on the image intensifier. System flow was 59 ml per min, and the contrast media consisted of 0.35 ml of Hypaque 50 injected over 1 sec. These raw data were used to investigate the effects of size, shape, and position of the region of interest (ROI) upon T-D curves and to determine the relative accuracy of averaged versus total data collection. In each case, the integrated area was calculated after a gamma-variate fit was applied to the T-D curve. The data used to make the gamma-variate curve ranged from the point at which the data rose to 20% of the peak density through the peak at which the data fell back to 40%. To study the effect of variables on the integrated area of the T-D curves, we repeated the DSA runs and changed one variable each time. The variables studied included kVp, mAs, frame rate, subject density, matrix size, and image-intensifier mode.

To determine the accuracy of flow measurements, we completed multiple DSA runs with
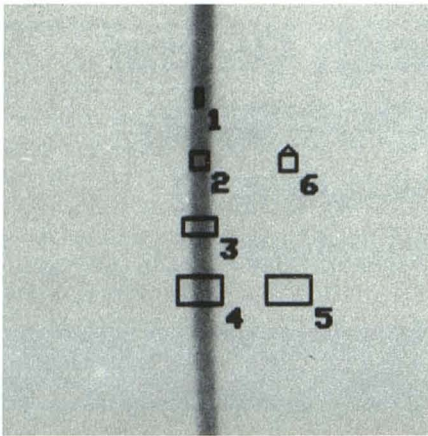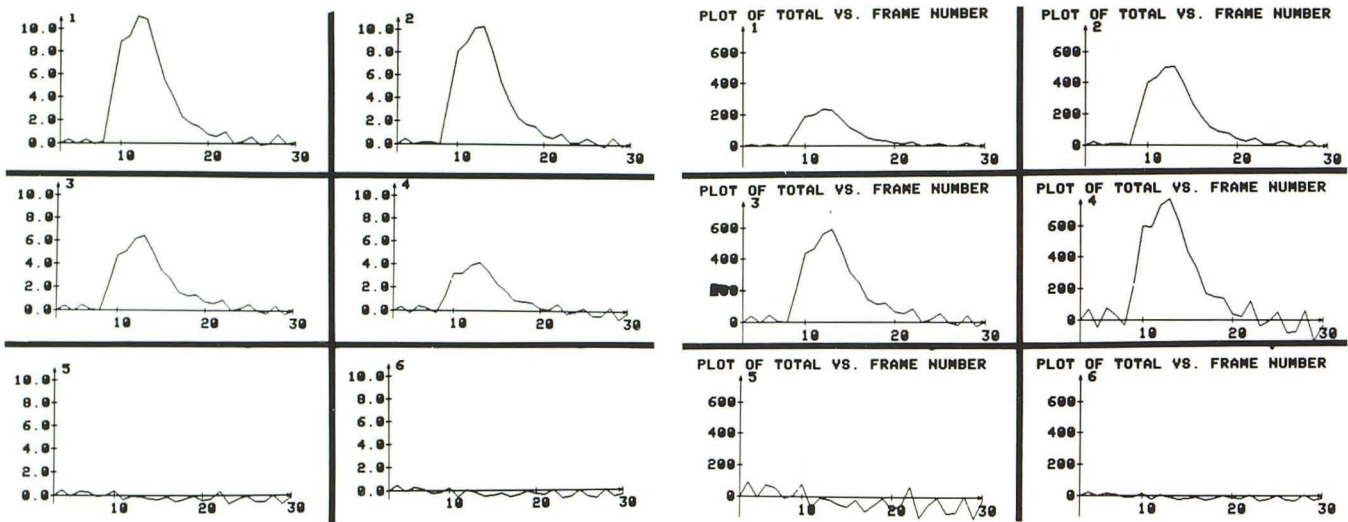
Fig. 1.—Time-density (T-D) curves were generated with different-sized regions of interest (A) using both averaged data (B) and total data (C). With larger ROIs, integrated curve area decreased for averaged data but increased for total data.

known flow values (ranging from 25 to 300 ml/min) and tubes of various diameters (2.3, 4.7, 6.2, and 7 mm). All other variables were kept constant.

Results

Methods of Accumulating T-D Curves

We selected a DSA run and placed different-sized ROI boxes on the model tube or vessel and background areas to evaluate the effect of ROI size on the flow curves for both averaged and total data (Fig. 1A). With averaged data, the T-D curves decreased as the size of the ROI was increased (Fig. 1B, curves 1 through 4). The amplitudes of the background (curves 5 and 6) were the same for the small and large ROIs. The reverse effect was observed with total data. The T-D curves increased in size as the ROI was increased (Fig. 1C, curves 1 through 4). Furthermore, the background amplitude was higher for the larger ROI (curves 5 and 6). Increasing the height of the ROI increased the T-D curve with total data but had no effect on averaged data.

With averaged data, the ROI was moved from side to side and longitudinally along the tube to measure the effect of ROI position. The diameter of the contrast column within the tube was approximately 5 pixels. When the ROI (1 × 2 pixels) was shifted 1 pixel to the left or right of center, there was a 2.8% decrease in integrated area under the T-D curve. A 2-pixel shift to either side resulted in a 5.5% decrease in curve area. When an ROI box (3 × 3 pixels) was placed in five locations along the tube, the SD of the integrated areas of the five T-D curves was ±3.1%.

Finally, T-D curves were generated for each of the 10 DSA runs with averaged data and total data to determine which method gave more accurate flow measurements. For averaged data, a 3 × 3 pixel ROI was placed within the model vessel, and for total data a 5 × 8 pixel ROI was positioned to include the entire width of the vessel. The background was subtracted in each case. Curve area was calculated by using a gamma-variate fit as described in the previous section. The % SD was ±4.49 for averaged data and ±6.85 for total data acquisition. The background density was approximately 5%
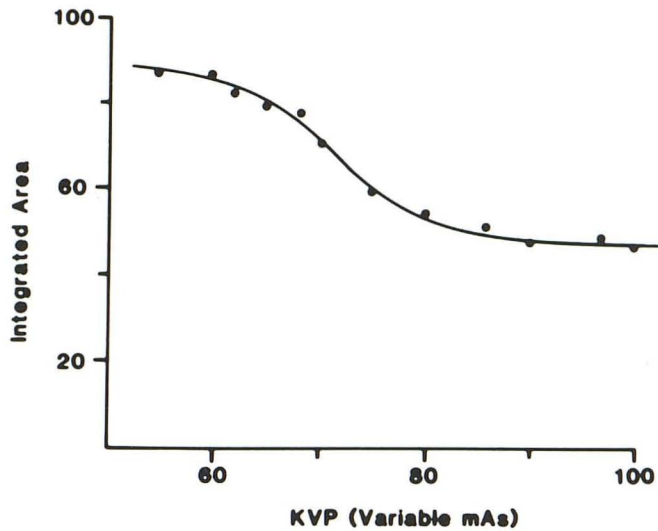
Fig. 2.—As kVp was varied from 55 to 100, the mAs was adjusted to maintain a constant exposure. As kVp increased, curve area decreased in a nonlinear fashion. Steeper negative slope between 65 and 75 kVp reflects k-edge of iodine with a polychromatic X-ray beam.

Fig. 3.—Comparison of calculated flow from the DSA curves with known (actual) flow values. Diagonal line represents the line of identity.

of the contrast density for the averaged data and 8% for the total data.

Technical Variables

A direct linear correlation was found between the framing rate and the integrated area of the T-D curves.

As the kVp was increased from 55 to 100, the integrated curve area progressively decreased, but not in a linear fashion. A distinct decline occurred between 65 and 75 kVp (Fig. 2). Changing the mAs with a constant kVp resulted in no change in the integated areas of the T-D curves.

A step-wedged phantom was placed over the model vessel to simulate subject density. The subject density had no observable effect upon the T-D curves.

Finally, the DSA runs were obtained with matrix sizes of 128, 256, and 512, and with the 4-, 6-, and 9-in. (10-, 12.5-, and 22.5-cm) modes on the image intensifier. Changing the matrix size of the image-intensifier mode had no observable effect upon the T-D curves.

Accuracy of DSA Transit Flow Measurements

Since $Q = [(A_v \, I)/A_c] \cdot k$, where Q = flow, A_v = cross-sectional area of the vessel, I = amount of iodine injected, A_c = integrated area of the T-D curve, the constant k can be determined if the flow is known. The constant k was determined to be 5.3. Using this constant, we calculated flow values from the multiple DSA runs obtained by varying flow and vessel size with other variables remaining constant. One set of data was excluded because it was entirely inconsistent with the others and could not be reproduced. A good correlation was noted between the known and calculated flow rates (r = 0.882) (Fig. 3).
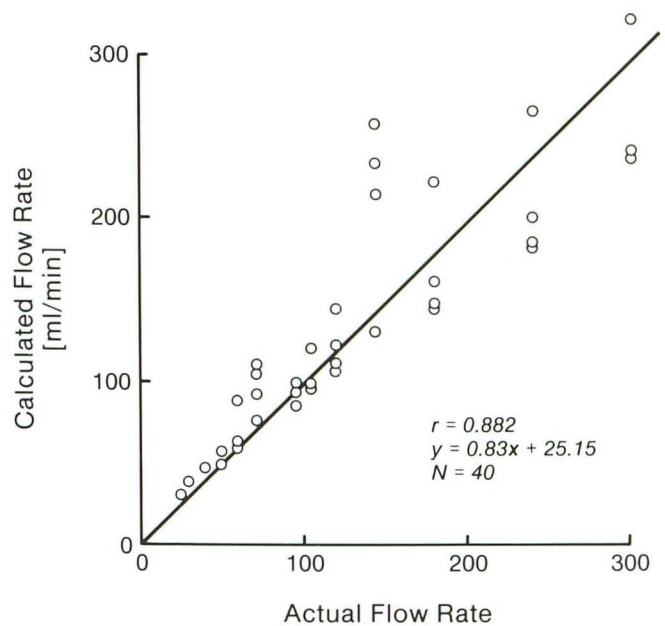
Discussion

Our results show that the method of data acquisition affects the T-D curves and the flow data. With averaged-data acquisition, the amplitudes of the T-D curves are inversely related to ROI size (Fig. 1B). This is to be expected because the density numbers of all the pixels within the ROI are added and the total is divided by the total number of pixels. Density is directly proportional to the thickness and concentration of the contrast material. Since the tube used in the experiments is round, the pixels near the edge of the vessel measure a smaller thickness of contrast material (Fig. 4). If the diameter of the ROI is greater than that of the tube, the pixels without contrast material are averaged with the pixels over the vessel, resulting in a lower number.

With total-data acquisition, the density numbers of all the pixels in the ROI are added together. Consequently, the amplitudes of the T-D curves increase as the size of the ROI increases (Fig. 1C). When the ROI extends beyond the tube, the amplitudes of T-D curves continue to increase because more background noise is added. As the background ROI increases, the amplitude of the background T-D curve increases, whereas with averaged data, the ROI size does not affect background curves.

Precise placement of the ROI over the tube is essential in averaged-data acquisition. With a cylindrical tube 5 pixels in diameter, a 1-pixel shift can result in underestimation of the integrated curve area by 2.8%. Since there is also some variation along the length of the tube, the ROI should be placed in the same region each time. A number of factors account for the regional variation: (1) regional differences in photon flux and field differences along the imaging chain, (2) variation in the inner diameter of the plastic tubing, (3) stream-
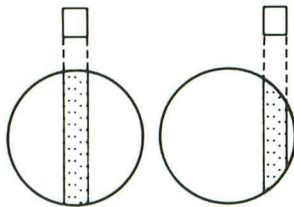
Fig. 4.—Thickness of contrast viewed by pixel. Centered pixel (**A**) thicker segment of contrast material than pixel near the edge (**B**) of round vessel. Density measurement of pixel in **A** would be higher than pixel in **B**.

ing or nonideal flow, (4) finite frame rate and, (5) off-center positioning of the ROI. With a finite frame rate, the system may sample slightly different portions of the contrast bolus curve. A faster framing rate or continuous-mode DSA system would be preferable. We were limited to a framing rate of 4 per sec because of a mechanical contact generator. With regard to positioning, the ROI moves only on whole-pixel shifts. Perfect centering of the ROI on the vessel would require a fractional pixel shift. This would be less of a problem with a larger matrix because the pixels are smaller.

Even after the contrast bolus passes the ROI, a tail in the T-D curve occurs because the density measurements do not return to baseline. This is caused by laminar flow and turbulence. In the former, contrast material is moving faster in the center of the vessel than adjacent to the wall, where it is relatively stagnant and lags behind the main bolus. On the other hand turbulence causes more mixing and dilution of contrast material, which leads to broadening of the T-D curve. Although there is uncertainty about how much of the tail should be included when the curve area is integrated, a gamma-variate fit produced the most consistent results.

More accurate results are obtained with averaged data acquisition. DSA systems are inherently noisy. Average data with a small ROI gives a higher signal-to-noise ratio. Background subtraction eliminates much, but not all, of the error caused by system noise, because system noise is random and varies across the field of view. Furthermore, with a small ROI, chance of including line-scan artifacts of the video system is less likely. The use of a small ROI has a practical advantage because less time is required to accumulate the data. In a clinical setting, there is less likelihood of including adjacent vessels when a small ROI is used and the data are less influenced by misregistration. The optimal method for acquisition of flow data with a Technicare DSA system is to: (1) place a small ROI over the vessel to be studied, (2) use averaged data, (3) apply background subtraction technique, and (4) integrate the curve area after a gamma-variate fit.

Erroneous flow data are avoided by recognizing and understanding the effects of radiographic exposure factors on T-D curves. Peak kilovoltage affects the density measurements because radiographic contrast varies inversely with kVp. Therefore, if the kVp is increased in DSA, the density difference between a vessel filled with contrast agent and the adjacent background decreases. As the density difference decreases, the integrated curve area also decreases. The rate of change of the integrated area is highest in the kVp range of 65–75 (Fig. 2), and the portion of the curve reflects the k-edge of iodine with a polychromatic X-ray beam.

One might expect that the mAs would also affect the DSA

density measurements, because changes in the mAs alter density on radiographic film, fluoroscopy, and videodensitometry [2]. However, the data show that mAs does not affect the T-D curves obtained with DSA. Our DSA system logarithmically amplifies the video signal and uses a subtraction technique. As shown in Figure 5, doubling the mAs results in doubling of the pixel amplitudes in both the mask and contrast frames. However, the difference of the logs of the pixel amplitudes is identical for the two mAs values. On the other hand, if a linear subtraction processing is used, the mAs will affect the DSA density measurements. Most DSA systems use logarithmic processing.

Increasing subject density does not directly affect flow measurements, but it does introduce error by contributing to beam hardening and scatter. Similarly, increasing field size contributes to scatter. As pointed out by Shaw et al. [3], beam hardening, X-ray scatter, and veiling glare are significant sources of error in DSA density measurements. All three factors suppress the iodine signal resulting in falsely low density measurements. The same group of investigators have reported a digital convolutional algorithm to correct for X-ray scattering and veiling glare [4].

Another source of error is imprecision in the measurement of the vessel diameter. A measurement error of 0.5 mm in a 5-mm vessel results in a 19% error in the flow calculation. Edge-detection algorithms have been developed for digital systems but were not useful for improving the accuracy of vessel measurement.

System drift was not a major problem in the DSA system. At least, density measurements of a phantom varied only by a % SD of ±4.3 over a 3-month period. Nevertheless, when flow values measured on different days are compared, it is advisable to standardize the measurements by determining the constant k on each day on which a flow study is to be done. Although our flow model is relatively simple, it does require time to set it up and thus would be impractical for that purpose. We have developed a mechanical flow model in our laboratory that could be conveniently used [5].

Measurement of the degree of arterial stenosis is less accurate on a digital image than on a conventional radiographic image because there is less spatial resolution in the former. However, determination of the degree of stenosis is imprecise even on conventional radiographs because the residual lumen can be measured on only one projection. Therefore, measuring the flow may be useful for establishing the presence of a hemodynamically significant lesion. Our results show good correlation between in vitro flow measurements made by DSA and actual flow rates.

Despite the demonstrated in vitro accuracy, measurement of flow with DSA systems has not yet gained clinical acceptance. This delay results from the multiple variables and sources of error, which cause uncertainty in individual flow measurements in a clinical setting. Some of the variables that affect absolute flow measurements can be eliminated by measuring relative flow rates [6]. However, these require injection of contrast media into both the aorta and selectively into the vessel to be studied. In this case, the values are given as percentages of cardiac output.

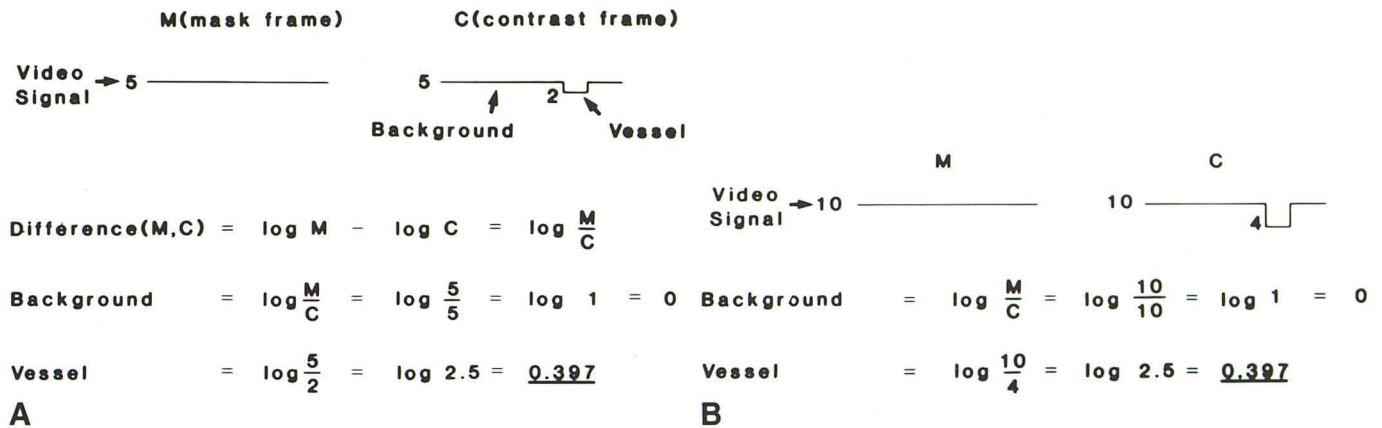All videodensitometric methods have limitations for assess-

M(mask frame)   **C(contrast frame)**

Video $\rightarrow 5$ ————————   5 ————————
Signal

                         Background   Vessel

Difference(M,C) = log M − log C = log $\frac{M}{C}$

                                                            Video $\rightarrow 10$ ———————— 10 ————————
                                                            Signal

Background = log $\frac{M}{C}$ = log $\frac{5}{5}$ = log 1 = 0   Background = log $\frac{M}{C}$ = log $\frac{10}{10}$ = log 1 = 0

Vessel = log $\frac{5}{2}$ = log 2.5 = **0.397**   Vessel = log $\frac{10}{4}$ = log 2.5 = **0.397**

A   **B**

Fig. 5.—Calculations for two different X-ray exposures. **A**, mAs_1; **B**, mAs_2 (= 2 mAs_1). Change in mAs does not affect DSA density measurements.

ing carotid artery disease. Whether these methods use relative or absolute measurements, only flow at the site of injection is determined. If the injection is made in the common carotid artery, flow can be determined for that vessel only and not for the internal carotid and external carotid arteries. Such information is of limited clinical value. A catheter must be selectively placed in the internal carotid artery if flow in that vessel is to be determined. This is hazardous in patients with disease of the carotid bifurcation, and flow determinations by this method are impossible.

REFERENCES

1. Hesselink JR, Chang KH, Chung KJ, Abbate L. Flow analysis with digital subtraction angiography: 1. description of a simplified flow model. *AJNR* **1986**;7:423–426
2. Lantz BMT, Foerster JM, Link DP, Holcroft JW. Determination of relative blood flow in single arteries: new video dilution technique. *AJR* **1980**;134:1161–1168
3. Shaw CG, Ergun DL, VanLysel MS, et al. Quantitation techniques in digital subtraction video angiography. *Digital Radiography* **1981**;314:121–129
4. Shaw CG, Ergun DL, Myerowitz PD, et al. Technique of scatter and glare correction for video densitometric studies in digital subtraction video angiography. *Radiology* **1982**;142:209–213
5. Goodsitt MM, Abbate L, Hesselink JR. A solid bolus contrast digital phantom for assessing the performance of digital subtraction angiography systems. *Radiology* (in press)
6. Lantz BMT, Dublin AB, McGahan JP, Link DP. Carotid blood flow in man determined by video dilution technique: I. Theory, procedure and normal values. *AJNR* **1981**;2:511–516